

SINR and Throughput Scaling in Ultradense Urban Cellular Networks

Abhishek K. Gupta, Xincheng Zhang, Jeffrey G. Andrews

Abstract—We consider a dense urban cellular network where the base stations (BSs) are stacked vertically as well as extending infinitely in the horizontal plane, resulting in a greater than two dimensional (2D) deployment. Using a dual-slope path loss model that is well supported empirically, we extend recent 2D coverage probability and potential throughput results to 3 dimensions. We prove that the “critical close-in path loss exponent” α_0 where SINR eventually decays to zero is equal to the dimensionality d , i.e. $\alpha_0 \leq 3$ results in an eventual SINR of 0 in a 3D network. We also show that the potential (i.e. best case) aggregate throughput decays to zero for $\alpha_0 < d/2$. Both of these scaling results also hold for the more realistic case that we term $3D^+$, where there are no BSs below the user, as in a dense urban network with the user on or near the ground.

I. INTRODUCTION

Cellular networks have been continually densifying their base stations (BSs) since their inception, driving most of the increased throughput over the past several decades [1]. The urban environments where spectrum is most scarce and high capacity most critical are themselves continually densifying, particularly vertically, albeit at a slower rate. Future cellular deployments, featuring small low power base stations, will extend in the vertical direction as well as in the 2D plane. Recently, [2] showed that for a 2D network, the coverage probability for a given SINR value decays to zero as the network is heavily densified if the close-in (i.e. within a distance R_c) path loss exponent α_0 is less than 2, regardless of the other path loss exponents outside R_c . The potential throughput, i.e. the best case aggregate throughput, still grows at-least sub-linearly if $\alpha_0 > 1$.

Other Related Work: The coverage probability of cellular wireless systems has been studied in detail in recent years using stochastic geometry [3], [4] for various 2D deployment scenarios. In [5], a general d dimensional Poisson Point Process (PPP) BS deployment is considered and an equivalent one dimensional (1D) PPP is derived to compute the SINR and rate coverage for highest instantaneous power based association. The dual-slope path loss model [6] is a generalization of standard single slope path loss model, which was analyzed in [2] and is the focus of this letter. It is well supported by many measurements [7], [8], [9] and shown to be very close to many scenarios of current interest including indoor [10], LTE [11], [12] and millimeter wave [13], [14].

A. K. Gupta (g.kr.abhishek@utexas.edu) and J. G. Andrews (jandrews@ece.utexas.edu) are with Wireless Networking and Communications Group, Department of Electrical and Computer Engineering at the University of Texas at Austin, Austin, TX 78712 USA. Xincheng Zhang is with Qualcomm Inc.

Contributions: The contribution of this letter is to extend [2] to three dimensions. The typical 3D case corresponds to a user sufficiently high off the ground in a dense urban environment that they see an appreciable number of BSs in every direction. We also consider a case we term $3D^+$, which is a special case of 3D with BSs extending overhead in the positive direction only, corresponding more closely to a user on the ground. We compute the probability of coverage (SINR distribution) and the potential throughput for both of these cases. Then we compute the critical values of the close-in path loss exponent for which SINR and throughput respectively go to zero as the density goes to infinity for both the 3D and $3D^+$ cases.

II. SYSTEM MODEL

We consider a downlink cellular network with BSs located in a d -dimensional space according to a Poisson Point Process (PPP) $\Phi = \{x_i : x_i \in \mathbb{R}^d\}$ with intensity λ . The average number of BSs in a d -ball of radius r located at origin for such a PPP is given by

$$\Lambda(\mathcal{B}(r)) = V_d r^d \lambda$$

where $V_d r^d$ is the volume of d -ball $\mathcal{B}(r)$ and V_d is a constant dependent on the dimension d . Note that $V_2 = \pi$ and $V_3 = \frac{4}{3}\pi$, while for the $3D^+$ case, BSs are located only in a half sphere, so $V_{3D^+} = V_3/2 = \frac{2}{3}\pi$. With a slight abuse of notation, we will use $d = 3D$ and $3D^+$ to differentiate between 3D and $3D^+$ cases where necessary, keeping in mind that $d = 3$ for both cases.

We assume a dual-slope path loss model which has two different path loss exponents, as in [2], given as

$$\ell(r) = \begin{cases} r^{-\alpha_0}, & \text{for } r \leq R_c \\ \eta r^{-\alpha_1}, & \text{for } r \geq R_c \end{cases},$$

where R_c is the critical distance, α_0 is the close-in path loss exponent and α_1 is the long-range path loss exponent, with $\eta = R_c^{\alpha_1 - \alpha_0}$ a constant to provide continuity. We require $0 \leq \alpha_0 \leq \alpha_1$, and assume Rayleigh fading for all links, therefore the received power at the origin from the i^{th} BS located at x_i is given by $P_i = h_i \ell(\|x_i\|)$, where h_i 's are i.i.d. exponential random variables with mean 1.

We assume that the user connects to the BS providing the highest average received power (i.e. closest BS) and denote this BS by index 0. Therefore the SINR is

$$\text{SINR} = \frac{h_0 \ell(\|x_0\|)}{\sigma^2 + \sum_{i \in \Phi \setminus \{0\}} h_i \ell(\|x_i\|)}$$

where σ^2 is the noise variance.

We are interested in the following two performance metrics.

Definition 1. The downlink coverage probability in d dimensions is

$$P_{\text{SINR}}^d(\lambda, T) = \mathbb{P}[\text{SINR} > T],$$

which is equivalently the ccdf of the SINR.

Definition 2. The potential throughput τ_l^d captures the average number of bits that can be transmitted per unit area per unit time per unit bandwidth, assuming all BSs transmit (i.e. full buffer model), and is

$$\tau_l^d(\lambda, T) = \log_2(1 + T) \lambda P_{\text{SINR}}^d(\lambda, T).$$

It has units of area spectral efficiency: bps/Hz/m².

III. PROBABILITY OF COVERAGE

In this section, we first derive the coverage probability expression for general path loss function and present the simplified expression for the dual-slope path loss model.

Lemma 1. The coverage probability with a general path loss function is

$$P_{\text{SINR}}^d(\lambda, T) = \lambda V_d \int_0^\infty e^{-T\sigma^2/\ell(y^{\frac{1}{d}})} \times \exp\left(-\lambda V_d y \left(1 + \int_1^\infty \frac{T}{T + \frac{\ell(y^{\frac{1}{d}})}{\ell((ty)^{\frac{1}{d}})}} dt\right)\right) dy. \quad (1)$$

For the 3D and 3D⁺ cases, V_d is $\frac{4\pi}{3}$ and $\frac{2\pi}{3}$, respectively.

Proof: See Appendix A. ■

We observe that expression for 3D and 3D⁺ are the same, except for the value of V_d . Also, the effective BS density for 3D⁺ is $\frac{\lambda}{2}$ when compared to the 3D case. Thus, from now on, we will consider only the 3D case for analysis with the understanding that such results can be trivially converted to 3D⁺. Fig. 1 validates Lemma 1 by comparing a simulation of the system model with the analytic expression given in the Lemma. It also shows that the SINR coverage of a 3D⁺ deployment with density λ is equal to that of a 3D deployment with density $\frac{\lambda}{2}$.

Lemma 1 can be further simplified for the dual-slope case to give the following Theorem.

Theorem 1. The downlink coverage probability for a general d -dimensional PPP BS deployment under the dual-slope model is given as

$$P_{\text{SINR}}^d(\lambda, T) = \lambda V_d R_c^d \int_0^1 e^{-\lambda V_d R_c^d I(T, r) - T\sigma^2 R_c^{\alpha_0} r^{\frac{\alpha_0}{d}}} dr + \lambda V_d R_c^d \int_1^\infty e^{-\lambda V_d R_c^d C(-\frac{\alpha_1}{d}, T) r - T\sigma^2 R_c^{\alpha_0} r^{\frac{\alpha_0}{d}}} dr \quad (2)$$

where

$$I(T, r) = C\left(\frac{\alpha_0}{d}, \frac{1}{Tr^{\frac{\alpha_0}{d}}}\right) + C\left(-\frac{\alpha_1}{d}, Tr^{\frac{\alpha_0}{d}}\right) - rC\left(\frac{\alpha_0}{d}, \frac{1}{T}\right) + r - 1, \\ C(b, z) = {}_2F_1\left(1, \frac{1}{b}, 1 + \frac{1}{b}, -z\right),$$

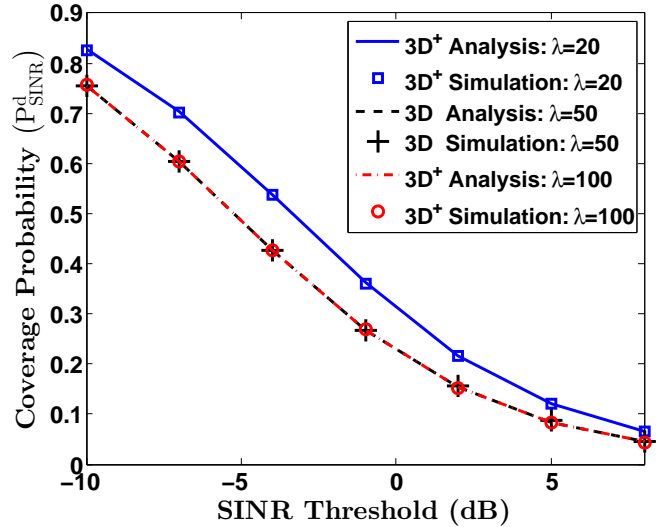


Fig. 1. SINR coverage probability for 3D⁺ and 3D BS deployment with $\alpha_0 = 3.3, \alpha_1 = 5, \sigma^2 = 1, R_c = 0.4$.

with ${}_2F_1(a, b, c, z)$ being the Gauss hypergeometric function.

Proof: See Appendix B. ■

Before going further, we will also compute the SIR coverage probability assuming noise to be zero which mimics the interference limited case. SIR coverage probability tightly upper bounds SINR coverage probability for dense deployments and is given as

$$P_{\text{SIR}}^d(\lambda, T) = \lambda V_d R_c^d \left(\int_0^1 e^{-\lambda V_d R_c^d I(T, r)} dr + \int_1^\infty e^{-\lambda V_d R_c^d C(-\frac{\alpha_1}{d}, T) r} dr \right) = \lambda V_d R_c^d \int_0^1 e^{-\lambda V_d R_c^d I(T, r)} dr + \frac{e^{-\lambda V_d R_c^d C(-\frac{\alpha_1}{d}, T)}}{C(-\frac{\alpha_1}{d}, T)}.$$

The SNR coverage probability can be found similarly by letting the interference go to zero.

The following Lemma establishes the relationship between the 2D case considered in [2] and the general d -dimensional case.

Lemma 2. The probability of (SIR, SINR and SNR) coverage for a general d dimension PPP BS deployment with parameters $\alpha_0, \alpha_1, \lambda, R_c, \sigma^2$ is equal to the probability of coverage for a 2D system with $\alpha'_0, \alpha'_1, \lambda', R_c, (\sigma')^2$ if

$$\alpha'_0 = \frac{2}{d}\alpha_0, \quad \alpha'_1 = \frac{2}{d}\alpha_1, \\ \lambda' = \frac{R_c^d V_d}{R_c^2 V_2} \lambda, \quad (\sigma')^2 = \sigma^2 R_c^{\alpha_0 - \alpha'_0}.$$

Proof: Proven easily by substituting the respective parameters in (2) for $d = 2$ and observing the exact same expression. ■

Following the similarity of SINR expression to that in [2], it can be shown that [2, Lemma 2] and [2, Theorem 2] will also be valid for the general d dimensional case. Building on these results and Lemma 2, we state the following Theorem.

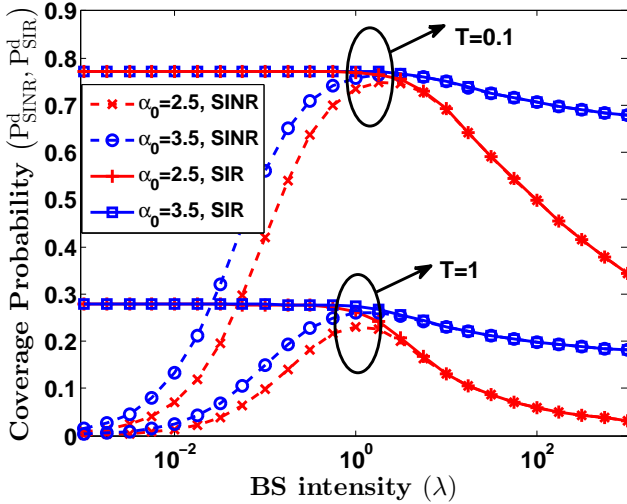


Fig. 2. SINR and SIR coverage scaling vs. network density (λ) for 3D deployment, with $\alpha_0 = [2.5, 3.5]$, $\alpha_1 = 4$, $R_c = 0.4$, $\sigma^2 = 1$.

Theorem 2. Under the dual-slope path-loss model, the SIR and SINR coverage probability of a general d -dimensional system go to 0 as $\lambda \rightarrow \infty$ for $\alpha_0 \leq d$.

Proof: See Appendix C. ■

The above Theorem is true for general d dimensional deployments and hence is valid for both the $3D^+$ and $3D$ cases. It provides the critical values of the close-in path loss exponent below which the coverage probability goes to zero. Theorem implies that for both the $3D$ and $3D^+$ scenario, the critical value of α_0 is 3. It is very common for the path loss exponent of short range systems to be less than these α_0 values, so this is seemingly an important concern for future ultra dense networks.

Fig. 2 shows the behavior of SINR and SIR coverage probability (P_{SINR}^{3D} and P_{SIR}^{3D}) for a 3D BS deployment as the network density varies. It can be observed that for all path loss exponents, P_{SINR}^{3D} first increases as λ increases. After a critical limit of λ , P_{SINR}^{3D} starts decreasing. For α_0 less than 3, P_{SINR}^{3D} goes to zero while for $\alpha_0 > 3$, P_{SINR}^{3D} asymptotically becomes a nonzero constant as $\lambda \rightarrow \infty$. For lower λ , P_{SIR}^{3D} corresponds to coverage probability for single slope path loss model with α_1 and for higher λ , P_{SIR}^{3D} corresponds to that with α_0 . We can observe that P_{SIR}^{3D} goes to zero for $\alpha_0 < 3$ as λ goes to infinity.

IV. POTENTIAL THROUGHPUT

We now turn to the potential throughput scaling with density.

Theorem 3. Under the dual-slope model, as $\lambda \rightarrow \infty$, the potential throughput τ_I^d

- 1) grows linearly with λ if $\alpha_0 > d$,
- 2) grows sublinearly with rate $\lambda^{(2-\frac{d}{\alpha_0})}$ if $\frac{d}{2} < \alpha_0 < d$,
- 3) decays to zero if $\alpha_0 < \frac{d}{2}$.

Proof: Using Lemma 2, we can prove that the potential throughput in a general d dimensional BS deployment is

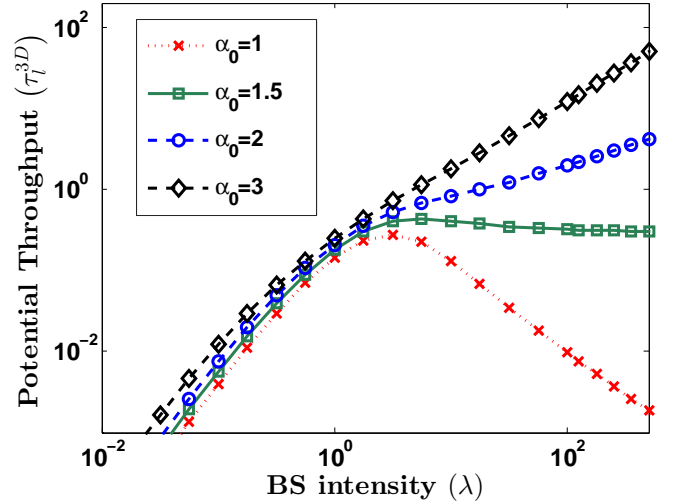


Fig. 3. Potential throughput (τ_I) scaling with network density for 3D deployment. Here, $\alpha_0 = [1, 1.5, 2, 3]$, $\alpha_1 = 4$, $R_c = 0.4$, $\sigma^2 = 1$, $T = 1$.

connected to that of 2D case by the following relation:

$$\tau_I^d(\lambda, T, \alpha_0, \alpha_1, R_c, \sigma^2) = \frac{R_c^2 V_2}{R_c^d V_d} \tau_I^{2D}(\lambda', T, \alpha_0', \alpha_1', R_c, (\sigma')^2).$$

Using the above relation and [2, Theorem 3], all three results of the Theorem 3 can be easily proven. For $\alpha_0 > d$, [2, Theorem 3] states that potential throughput in 2D case scales linearly with λ' for $\alpha_0' > 2$. Therefore, the potential throughput in the general d -dimensional case will scale linearly with λ if $\alpha = \alpha_0' \frac{d}{2} > d$. Similarly, the other two results for $\frac{d}{2} < \alpha_0 < d$ and $\alpha_0 < \frac{d}{2}$ can be obtained. ■

Fig. 3 shows the scaling of potential throughput with respect to λ for a 3D deployment. As expected, for $1.5 < \alpha_0 < 3$ the potential throughput scales only sub-linearly. Theorem 3 provides a theoretical basis for understanding the gain in throughput vs. the cost of densification.

We conclude by noting that the SINR throughput and SINR scaling results can be easily extended to more than two path loss exponents. Owing to the equivalency between the 2D case discussed in [2] and the general d dimensional case, Theorem 2 and Theorem 3 can be shown to be true for the multi-slope path loss model also.

APPENDIX A PROOF OF LEMMA 1

Let us denote the sum interference at origin by I . Now the SINR coverage probability can be written as

$$\begin{aligned} P_{\text{SINR}}^d &= \mathbb{P}[\text{SINR} > T] = \mathbb{P}\left[\frac{h_0 \ell(\|x_0\|)}{\sigma^2 + I} > T\right] \\ &= \int_0^\infty e^{-T\sigma^2/\ell(x)} \mathcal{L}_I(T/\ell(x)) f_{\|x_0\|}(x) dx \end{aligned} \quad (3)$$

where $f_{\|x_0\|}(x)$ is the probability distribution of the distance $\|x_0\|$ of the closest (serving) BS from origin given as $f_{\|x_0\|}(x) = V_d d \lambda x^{d-1} e^{-\lambda V_d x^d}$ and $\mathcal{L}_I(s)$ is the Laplace

transform of interference which can be derived as

$$\begin{aligned}\mathcal{L}_I(s) &= \mathbb{E} [e^{-sI}] = \mathbb{E} \left[e^{-s \sum_{z \in \Phi, \|z\| > x} h_z \ell(\|z\|)} \right] \\ &= \exp \left(-\lambda \int_x^\infty \frac{s \ell(z)}{1 + s \ell(z)} V_d dz^{d-1} dz \right).\end{aligned}$$

Substituting the values of $f_{\|x_0\|}(x)$ and $\mathcal{L}_I(s)$ in (3), we get

$$\begin{aligned}P_{\text{SINR}}^d &= V_d d \lambda \int_0^\infty e^{-T \sigma^2 / \ell(x)} x^{d-1} e^{-\lambda V_d x^d} \\ &\quad \exp \left(-\lambda \int_x^\infty \frac{\ell(z) T / \ell(x)}{1 + \ell(z) T / \ell(x)} V_d dz^{d-1} dz \right) dx \\ &\stackrel{(a)}{=} V_d d \lambda \int_0^\infty e^{-T \sigma^2 / \ell(x)} x^{d-1} e^{-\lambda V_d x^d} \\ &\quad \exp \left(-\lambda V_d x^d \int_1^\infty \frac{T}{\ell(x) / \ell(ux) + T} u^{d-1} du \right) dx\end{aligned}$$

where (a) is due to the substitution $z/x \rightarrow u$. Now using the substitutions $x^d \rightarrow y$ and $u^d \rightarrow t$, we get (1).

APPENDIX B PROOF OF THEOREM 1

Using the substitution, $r = y/R_c^d$ in (1), we get

$$\begin{aligned}P_{\text{SINR}}^d(\lambda, T) &= \lambda V_d R_c^d \int_0^\infty e^{-T \sigma^2 / \ell(R_c r^{\frac{1}{d}})} \\ &\quad \times \exp \left(-\lambda V_d R_c^d r \left(1 + \int_1^\infty \frac{T}{T + \frac{\ell(R_c r^{\frac{1}{d}})}{\ell(R_c (tr)^{\frac{1}{d}})}} dt \right) \right) dr.\end{aligned}\quad (4)$$

Outer integration from $r = 0$ to ∞ in (4) can be divided into integration over the following two intervals:

1) *In interval* $[0, 1)$: the inner integral can be written as

$$\begin{aligned}&\int_1^{\frac{1}{r}} \frac{T}{T + t^{\frac{\alpha_0}{d}}} dt + \int_{\frac{1}{r}}^\infty \frac{T}{T + t^{\frac{\alpha_0}{d}} r^{-\frac{\alpha_1 - \alpha_0}{d}}} dt \\ &= 1 + \frac{1}{r} C \left(\frac{\alpha_0}{d}, \frac{1}{T r^{\frac{\alpha_0}{d}}} \right) - C \left(\frac{\alpha_0}{d}, \frac{1}{T} \right) \\ &\quad + \frac{1}{r} C \left(-\frac{\alpha_1}{d}, -T r^{\frac{\alpha_1}{d}} r^{-\frac{\alpha_1 - \alpha_0}{d}} \right) - \frac{1}{r}.\end{aligned}\quad (5)$$

2) *In interval* $[1, \infty)$: the inner integral can be written as

$$\int_1^\infty \frac{T}{T + t^{\frac{\alpha_0}{d}}} dt = C \left(-\frac{\alpha_0}{d}, T \right) - 1.\quad (6)$$

Using (5) and (6) in (4), we get (2).

APPENDIX C PROOF OF THEOREM 2

This proof is similar to the proof of Proposition 1 in [2]. As the SINR coverage probability is always less than SIR coverage probability, it suffices to show the proof for SIR only. Using Lemma 1 and taking $\sigma^2 = 0$, we can upper bound the

SIR coverage probability as following: $P_{\text{SIR}}^d(\lambda, T)$

$$\begin{aligned}&\leq \lambda V_d \int_0^\infty \exp \left(-\lambda V_d y \left(1 + \int_1^{\max(1, \frac{R_c^d}{y})} \frac{T}{T + \frac{\ell(y^{\frac{1}{d}})}{\ell((ty)^{\frac{1}{d}})}} dt \right) \right) dy \\ &\quad + \lambda V_d \int_0^{R_c^d} e^{-\lambda V_d y} dy \\ &= \lambda V_d R_c^d \int_0^1 \exp \left(-\lambda V_d R_c^d y \left(1 + \int_1^{\frac{1}{y}} \frac{T}{T + t^{\frac{\alpha_0}{d}}} dt \right) \right) dy \\ &\quad + e^{-\lambda V_d R_c^d}.\end{aligned}$$

The second term goes to zero as $\lambda \rightarrow 0$. To prove the same for first term, consider an increasing sequence $\{\lambda_n\}$, and define

$$f_n(x) = \lambda_n \exp \left(-\lambda_n V_d R_c^d y \left(1 + \int_1^{\frac{1}{y}} \frac{T}{T + t^{\frac{\alpha_0}{d}}} dt \right) \right).$$

It is clear that $f_n(x) \rightarrow 0$ pointwise for each x in $(0, 1)$. Also,

$$f_n(x) \leq g(x) = \frac{1}{V_d R_c^d e \left(1 + \int_1^{\frac{1}{y}} \frac{T}{T + t^{\frac{\alpha_0}{d}}} dt \right)}.$$

$g(x)$ is integrable on $(0, 1)$ for $0 \leq \alpha_0 < d$. So by the dominance convergence theorem, first term, and hence the sum also goes to zero which proves the Theorem.

REFERENCES

- [1] J. Andrews, S. Buzzi, W. Choi, S. Hanly, A. Lozano, A. Soong, and J. Zhang, "What will 5G be?" *IEEE J. Sel. Areas Commun.*, vol. 32, no. 6, pp. 1065–1082, June 2014.
- [2] X. Zhang and J. Andrews, "Downlink cellular network analysis with multi-slope path loss models," *IEEE Trans. Commun.*, vol. 63, no. 5, pp. 1881–1894, May 2015.
- [3] J. Andrews, F. Baccelli, and R. Ganti, "A tractable approach to coverage and rate in cellular networks," *IEEE Trans. Commun.*, vol. 59, no. 11, pp. 3122–3134, Nov. 2011.
- [4] T. Bai and R. W. Heath Jr., "Coverage and rate analysis for millimeter wave cellular networks," *IEEE Trans. Wireless Commun.*, vol. 14, no. 2, pp. 1100–1114, Feb. 2015.
- [5] P. Madhusudhanan, J. Restrepo, Y. Liu, T. Brown, and K. Baker, "Downlink performance analysis for a generalized shotgun cellular system," *IEEE Trans. Wireless Commun.*, vol. 13, no. 12, pp. 6684–6696, Dec. 2014.
- [6] T. Sarkar, Z. Ji, K. Kim, A. Medouri, and M. Salazar-Palma, "A survey of various propagation models for mobile communication," *IEEE Antennas Propag. Mag.*, vol. 45, no. 3, pp. 51–82, June 2003.
- [7] V. Erceg, S. Ghassemzadeh, M. Taylor, D. Li, and D. Schilling, "Urban/suburban out-of-sight propagation modeling," *IEEE Commun. Mag.*, vol. 30, no. 6, pp. 56–61, June 1992.
- [8] M. Feuerstein, K. Blackard, T. Rappaport, S. Seidel, and H. Xia, "Path loss, delay spread, and outage models as functions of antenna height for microcellular system design," *IEEE Trans. Veh. Technol.*, vol. 43, no. 3, pp. 487–498, Aug. 1994.
- [9] J. R. Hampton, N. Merheb, W. Lain, D. Paunil, R. Shuford, and W. Kasch, "Urban propagation measurements for ground based communication in the military UHF band," *IEEE Trans. Antennas Propag.*, vol. 54, no. 2, pp. 644–654, Feb. 2006.
- [10] H. Hashemi, "The indoor radio propagation channel," *Proc. IEEE*, vol. 81, no. 7, pp. 943–68, Jul. 1993.
- [11] 3GPP 3GPP TR 36814-900, "Further advancements for E-UTRA - physical layer aspects (rel. 9)," 3GPP FTP Server, 2010.
- [12] P. Kyösti *et al.*, "WINNER II channel models," EC FP6, Tech. Rep., Sept. 2007.
- [13] T. Rappaport *et al.*, "Millimeter wave mobile communications for 5G cellular: It will work!" *IEEE Access*, vol. 1, pp. 335–349, 2013.
- [14] Y. Chang, S. Baek, S. Hur, M. Y., and Y. Lee, "A novel dual-slope mmWave channel model based on 3D ray-tracing in urban environments," in *IEEE PIMRC*, Sept. 2014.